Available online at www.sciencedirect.com
ScienceDirect
Journal of Organometallic Chemistry 692 (2007) 3261–3266
Journal of Organometallic Chemistry
www.elsevier.com/locate/jorganchem

Microviscosity and wavelength effects on radical cage pair recombination

John D. Harris, Alan B. Oelkers, David R. Tyler *

Department of Chemistry, University of Oregon, Eugene, OR 97403, United States

Received 5 January 2007; received in revised form 23 March 2007; accepted 23 March 2007
Available online 30 March 2007

Abstract

This study probed two aspects of the reactivity of geminate radical cage pairs formed by photolysis of $Cp'_2Mo_2(CO)_6$ ($Cp' = \eta^5$-$C_5H_4CH_3$). The first aspect studied examined whether the bulk viscosity has any predictive power in determining the magnitude of the cage recombination efficiency (F_{cP}). Although there is a clear relationship between the magnitude of F_{cP} and viscosity for systems where the bulk viscosity of the solution is altered by the addition of a non-macroscopic viscosity enhancer, the relationship is unclear for systems where the bulk viscosity is altered using polymeric viscosity enhancers. For this investigation, F_{cP} values were measured using femtosecond pump–probe transient absorption spectroscopy. The results clearly indicate that bulk viscosity can change drastically without affecting F_{cP} in systems containing small amounts of added polymers. The bulk viscosity is thus a poor parameter for predicting the cage effect in such systems. The second investigation looked at the effect of the photochemical excitation energy on F_{cP} for the $[Cp'(CO)_3Mo^{\cdot}, {}^{\cdot}MoCp'(CO)_3]$ cage pair in hexane. The results showed that F_{cP} increased when the wavelength of irradiation was changed from 546 nm to 436 nm, and then remained constant as the wavelength of irradiation was changed from 436 nm to 404 nm to 366 nm. These results are somewhat surprising because the recombination efficiencies for diatomic and triatomic molecules have been shown to decrease monotonically with increasing excitation energy. Two explanations are offered for the reverse wavelength dependence observed in this study. The first explanation invokes the different dynamic behaviors of the two excited states involved at the selected wavelengths, and the second invokes the different speeds of radical separation following irradiation at the selected wavelengths.

Keywords: Cage effect; Microviscosity; Pump–probe; Organometallic radicals; Photochemistry

1. Introduction

The solvent cage effect is vital to understanding the reactivity of radicals generated by bond homolysis reactions in solution [1–3]. The term ''cage effect'' refers to the phenomenon that the probability of recombination of a radical pair is greater in solution than in the gas phase. The origin of this effect is the solvent ''cage,'' a term introduced by Franck and Rabinowitch in 1934 for a hole in the solvent that temporarily traps a pair of reactive molecules causing them to remain as colliding neighbors for a short period of time before random motion allows their separation [4]. The photolysis of a generic dimer in solution to yield a cage pair is shown in Scheme 1.

Three different types of cage effects are generally recognized [5]: (1) Primary cage effects are those in which the geminate radicals recombine to reform the parent molecule before cage escape occurs. (2) Secondary cage effects are those in which the geminate radicals recombine to reform the parent molecules after cage escape has occurred but before a random distribution of the radicals in solution is achieved. The probability for this type of recombination decreases with increasing distance between the geminate radicals. (3) Cage effects involving non-geminate radicals (so-called ''encounter'' cage pairs) are those in which free

* Corresponding author.
E-mail address: dtyler@uoregon.edu (D.R. Tyler).

0022-328X/$ - see front matter © 2007 Elsevier B.V. All rights reserved.
doi:10.1016/j.jorganchem.2007.03.036

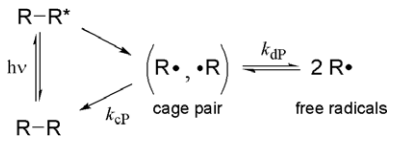

Scheme 1. The photolysis of a generic dimer in solution to yield a radical cage pair. The radicals in the solvent cage can either diffuse apart to yield free radicals or recombine to reform the parent dimer. The rate constants k_{cP} and k_{dP} are for radical–radical recombination and for radical diffusion out of the cage, respectively.

radicals diffuse together to combine and form a molecule [6].

Cage effects are quantitatively assessed by the cage recombination efficiency (F_{cP}), or the fraction of radical cage pairs which ultimately recombine, defined as the ratio of the rate constant for cage recombination to the sum of the rate constants for all competing cage processes [5]. In Scheme 1, $F_{cP} = k_{cP}/(k_{cP} + k_{dP})$, where the rate constants k_{cP} and k_{dP} represent the rates of recombination and diffusion, respectively, and the "P" subscript is used to indicate that the radicals were generated photochemically. Experimental work on I_2, Br_2, and Cl_2 in rare gas matrices and on I_2 in solution showed a linear dependence of F_{cP} on the wavelength of irradiation [6]. The accepted explanation of this phenomenon is that caged radical pairs formed by photolysis using higher energy light are created with a greater initial separation between the two radical fragments, as irradiation energy in excess of the bond dissociation energy is partitioned into kinetic energy of the atomic fragments. This leads to a lower recombination efficiency because recombination is less likely as the distance of initial separation increases [7]. Similar results were also obtained for the photodissociation of the simple triatomic molecules OClO and ClOH, where it was theorized that the majority of excess energy is converted into the translational motion of the radicals fragments, with little energy going to vibrational excitation [7]. It is not clear, however, if this same dependence of F_{cP} on wavelength holds for larger polyatomic molecules because energy transfer to the large number of vibrational modes available in such molecules may be very fast. To investigate this question, we studied the dependence of F_{cP} on the irradiation wavelength for the [Cp′(CO)$_3$Mo•, •MoCp′(CO)$_3$] radical cage pair, generated by photolysis of Cp′$_2$Mo$_2$(CO)$_6$ (Scheme 2). The results of our study are reported herein. Also reported are the results of a study to probe the effect that macromolecular viscosity enhancers have on F_{cP}. Bulk viscosity is generally seen as a variable with a very strong positive correlation to F_{cP} in solvent cage reactions, but, depending on the solvent composition, this relationship may not be universal. For example, the bulk viscosity of a solution may be easily manipulated through the addition of a small concentration of macromolecules, which would seemingly leave the molecular solvent properties surrounding a solvent cage pair largely unaltered. In such cases, it is not known whether the bulk viscosity has any predictive power in determining the magnitude of F_{cP}. In this study, this question is examined through a comparison of the empirically measured F_{cP} for similar solvent compositions with and without the addition of highly viscous macromolecular solutes.

2. Experimental

2.1. Instrumentation and reagents

All manipulations were carried out in the absence of water and atmospheric oxygen using standard glove box techniques. Due to the light-sensitive nature of the organometallic complex, all samples were prepared in the darkroom. Cp′$_2$Mo$_2$(CO)$_6$ was synthesized and purified as described in the literature [8]. THF (Fischer), Hexane (Fischer), and carbon tetrachloride (Aldrich) were purified according to standard literature techniques [9]. HPLC grade methanol (Aldrich), tetraethylene glycol dimethyl ether (tetraglyme; Aldrich), polyvinyl acetate (average MW 113,000; Aldrich), and squalane (Alfa Aesar) were used as received. Molecular sieves (4 Å) were added to all the solvents, which were stored in a darkened glove box. A Hewlett Packard 8453 UV–vis spectrophotometer was used for all of the electronic absorption spectra.

2.2. F_{cp} obtained from quantum yields as a function of viscosity

An Oriel Merlin radiometry system was used to monitor the photoreactions, which consists of: (1) an Oriel 200 W high pressure mercury arc lamp, (2) an Oriel 100 mm^2, NIST calibrated silicon photodiode (model 70356) detector, (3) an Oriel Merlin™ radiometer control unit, and (4) an IBM personal computer. The concentration of Cp′$_2$Mo$_2$(CO)$_6$ was changed for each experimental wavelength ($\lambda = 546$ nm, $\lambda = 436$ nm, $\lambda = 404$ nm, and $\lambda = 366$ nm) so that the resultant solutions had an absorbance

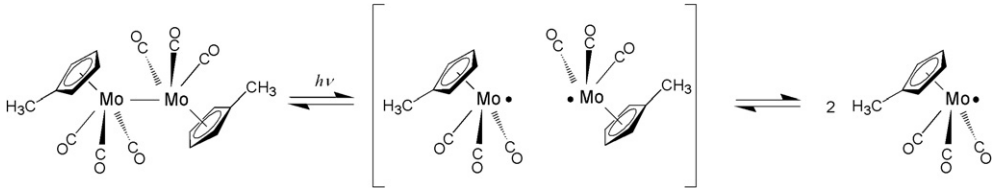

Scheme 2. Photolysis of Cp′$_2$Mo$_2$(CO)$_6$ leads to Cp′Mo(CO)$_3$ radicals by way of a [Cp′(CO)$_3$Mo•, •MoCp′(CO)$_3$] cage pair.

between 0.8 and 1.5. All of the solutions contained 80% (v/v) of the hexane/squalane solvent system, used to vary the viscosity, and 20% (v/v) carbon tetrachloride, used as the radical trap. During the experiment, the solutions were maintained at a constant 25.0 ± 0.1 °C. The absolute viscosities of the samples were measured in triplicate using calibrated Cannon-Fenske viscometers. The temperature of both the viscometer and solutions were equilibrated in a water bath (25.0 ± 0.1 °C) for 10 min before each measurement.

2.3. Femtosecond transient absorption spectroscopy

The full details of the femtosecond laser system and experimental design have been described [10]. Briefly, the master oscillator is a home-built, passively mode-locked Ti:Sapphire oscillator, pumped with a continuous wave (cw) frequency-doubled Nd:YLF laser (Spectra-Physics Millenia). The femtosecond oscillator produces a train of ca. 100 fs pulses at an 80 MHz repetition frequency and central wavelength of 800 nm. The oscillator output is directed into a stretched-chirped pulse regenerative amplifier (Spectra-Physics Spitfire). The regenerative amplifier is pumped by a Q-switched (1 kHz) frequency-doubled Nd:YVO_4 laser (Spectra-Physics Evolution). The amplifier produces a 1 kHz pulse train of 100 fs pulses with frequency centered at 800 nm, and total energy of 1 W (1 mJ/pulse). The amplifier output is split into probe and pump pulse trains using a thin dielectric beamsplitter. The pump pulse train with 515 nm wavelength is generated by optical parametric amplification (OPA) (Spectra-Physics). The probe pulse train is generated as the second harmonic of the 800 nm fundamental using a 0.5 mm type II β-barium borate (BBO) crystal. A paired-prism pulse compressor is used to eliminate second-order chirp in both pump and probe pulse trains in an effort to maintain the minimum time-bandwidth product at the sample interface. In order to collect isotropic data, the polarization of the pump pulse train is rotated to the magic angle (54.7°) with respect to the probe pulse using a broadband $\lambda/2$ waveplate and a thin film polarizer. The probe pulse is temporally delayed by a mechanical translation stage (Aerotech ATS-2060). The differential absorption of the systems studied was obtained by modulating the pump repetition frequency to 500 Hz, or 1/2 the probe repetition rate, using a mechanical chopper. The pump and probe pulses are focused to a diameter of 500 μm and 200 μm, respectively, at the flow cell interface, where the spot size measurement and the alignment of the pump and probe beams was achieved through the use of a set of precision-mounted pinhole apertures. The pump and probe pulse energies were approximately 8 and 0.5 μJ, respectively and the transient signal was found to be linear with pump power, indicating a one-photon process. Data was collected using a biased photodiode (Thorlabs DET-210), sampled with a boxcar averager (SRS-SR250) and transferred to a computer through an A/D converter. Accurate synchronization is obtained by indexing the probe signal to the 500 Hz pump signal, collected with a separate photodiode and boxcar set.

Because the compounds studied are air sensitive, the flow cell system was designed to be anaerobic. The flow cell system consists of a stainless-steel reservoir, a magnetically driven inert-fluid mechanical pump, stainless-steel tubing, and a custom-built stainless-steel flow cell with 1 mm thick CaF_2 windows and a 500 μm pathlength. The flow cell system was leak-checked under vacuum, and all solutions were deoxygenated prior to loading in the reservoir. The integrity of the studied samples was confirmed after laser studies by UV–vis absorption.

3. Results and discussion

3.1. Photochemistry

The electronic absorption spectrum of $Cp'_2Mo_2(CO)_6$ has two bands in the visible region (Fig. 1). The accepted interpretation of the electronic spectrum and photochemistry of this complex was originally provided by Wrighton and Ginley [11], who assigned the band at $\lambda_{max} = 390$ nm to a $\sigma \rightarrow \sigma^*$ transition and the band at $\lambda_{max} = 515$ nm to a $d\pi \rightarrow \sigma^*$-type transition [12]. In solution, irradiation into either absorption band causes Mo–Mo photolysis to form a [$Cp'(CO)_3Mo^{\bullet}$, $^{\bullet}MoCp'(CO)_3$] cage pair followed by formation of $Cp'Mo(CO)_3$ free radicals (Scheme 2) [3]. Mo–CO bond dissociation also occurs when the 390 nm band is irradiated [12], but it is noted that the steady-state method for determining F_{cP} is independent of side reactions [3] and consequently the presence of a Mo–CO bond dissociation process does not affect the accurate determination of F_{cP} values for the radical cage pairs formed by Mo–Mo bond homolysis [13]. In the presence of CCl_4, the $Cp'(CO)_3Mo^{\bullet}$ free radicals react to form $Cp'(CO)_3MoCl$ (Eq. (1))

$$Cp'_2Mo_2(CO)_6 \xrightarrow[\text{hexanes/squalane}]{h\nu(546\text{ nm})CCl_4} 2Cp'Mo(CO)_3Cl + 2[CCl_3^{\bullet}] \quad (1)$$

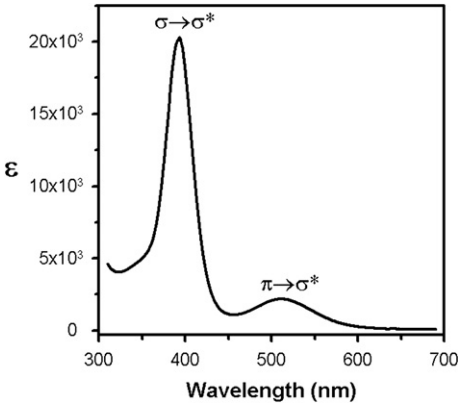

Fig. 1. The electronic absorption spectrum of $[Cp'Mo(CO)_3]_2$ in hexane. The annotations show the transition assignments of the absorption bands.

3.2. Measuring F_{cP}

The recombination efficiencies (F_{cP}) were measured in this study using two different experimental techniques. A steady-state photochemical technique was used to investigate the effect of irradiation wavelength on F_{cP}. This method obtains F_{cP} by measuring quantum yields for the radical trapping reaction with CCl_4 as a function of solvent viscosity (Eq. (1)). Femtosecond pump–probe transient absorption spectroscopy was used to investigate the effect of macromolecular viscogens on F_{cP}. This direct spectroscopic technique is essential for this investigation because the steady-state technique relies on viscosity-specific measurements to extract F_{cP}. Prior pump–probe experiments showed that primary cage effects for $Cp'_2Mo_2(CO)_6$ occurred on the 5 ps timescale but secondary and non-geminate cage effects for $Cp'_2Mo_2(CO)_6$ occurred on a time scale longer than 4000 ps [10]. In contrast, the steady-state method measures net F_{cP} values that are a combination of both primary and secondary caging. Non-geminate cage effects are effectively eliminated from the steady-state method by trapping all free radicals with an excess of CCl_4 [3].

3.3. The effect of macroscopic viscogens on F_{cP}

The effect of macroscopic viscogens on F_{cP} following homolysis of $Cp'_2Mo_2(CO)_6$ was investigated with a two-color femtosecond pump–probe transient absorption experiment. Specifically, F_{cP} was determined by monitoring the parent dimer population kinetics following Mo–Mo bond homolysis. To this end, a pump wavelength of 515 nm ($d\pi \rightarrow \sigma^*$) was used to selectively homolyze the Mo–Mo bond and generate [$Cp'(CO)_3Mo^{\bullet}$, $^{\bullet}MoCp'(CO)_3$] geminate radical pairs, and a probe wavelength of 400 nm, corresponding to the intense parent absorption band ($\sigma \rightarrow \sigma^*$), was used to observe the recombination kinetics . The kinetic transients collected from this experiment are a measurement of the parent dimer population kinetics following the pump-induced photolysis of the Mo–Mo bond (Fig. 1). The kinetic traces were found to fit satisfactorily to a bi-exponential function (Eq. (2))

$$\Delta A = [A_1(1 - \exp(-t/\tau_1)) + A_2(1 - \exp(-t/\tau_2)) + A_3] \times \mathrm{IRF} \quad (2)$$

in which ΔA represents the time-dependent differential absorption, A_1 and A_2 are the pre-exponential factors for the respective exponential rise-to-max functions with time constants τ_1 and τ_2 ($\tau^{-1} = k$) and A_3 is the non-decaying component representing the proportion of un-recovered bleach within the experimental timescale (ca. 4 ns). The kinetic equation is convoluted with the instrument response function (IRF) to fit the earliest-time dynamics adequately (Eq. (3))

$$\mathrm{IRF} = \frac{1}{2}\left[1 + \mathrm{erf}\left(\frac{t - \Delta t}{1.414\sigma}\right)\right] \quad (3)$$

This form is chosen to describe a Gaussian temporal profile, where erf(x) is the error function with a width parameter, σ, independently determined from a cross-correlation measurement.

The empirically measured kinetics have been interpreted to represent geminate recombination ($\tau_1^{-1} \approx 5\ \mathrm{ps} = k_1^{-1} = k_{cP}^{-1} + k_{dP}^{-1}$) and the subsequent vibrational relaxation of the newly reformed parent dimer ($\tau_2 \approx 100$ ps). Based on this model, the cage efficiency factor, F_{cP}, can be extracted from the empirical data fit using the following expression (Eq. (4)) [14]

$$F_{cP} = \frac{k_{cP}}{k_{cP} + k_{dP}} = -\frac{A_1 + A_2}{A_3} \quad (4)$$

A suitable test of the influence of macromolecular viscogens was found in the methanol/polyvinyl acetate solvent system. This solvent system was chosen because the $Cp'_2Mo_2(CO)_6$ and polyvinyl acetate were both soluble in methanol and because control experiments showed that the solvent system was inert to photochemical reactivity. The kinetic traces obtained from the pump–probe spectroscopic analysis of a methanol solution containing 0.1 M $Cp'_2Mo_2(CO)_6$ and a similar solution also containing 1% polyvinyl acetate are shown in Fig. 2. The similarity of the kinetic traces in Fig. 2 indicates that the added macromolecular viscogen has no effect on the observed kinetics. The F_{cP} values were extracted from these kinetic traces using the methods outlined above and gave for each case a value $F_{cP} = 0.33 \pm 0.01$. A significant difference was found, however, for the measured macroviscosity of these samples. The viscosity of the MeOH/$Cp'_2Mo_2(CO)_6$ solution was $\eta = 0.63 \pm 0.03$ cP, while that of the MeOH/$Cp'_2Mo_2(CO)_6$/1% polyvinyl acetate was $\eta = 1.03 \pm 0.04$ cP. Based on prior work in our laboratory, a change in η by 0.4 in this viscosity region should change

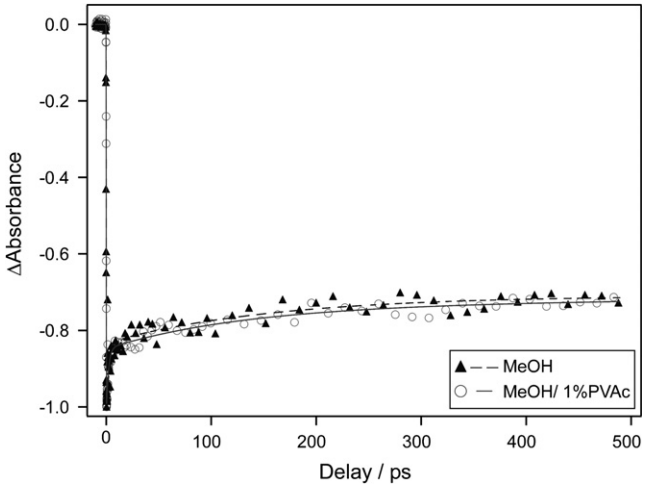

Fig. 2. Femtosecond pump–probe transient-absorption kinetic traces of $Cp'_2Mo_2(CO)_6$. The kinetic traces display a transient bleach and partial recovery at $\lambda_{probe} = 400$ nm following photolysis at $\lambda_{pump} = 515$ nm. The solvent compositions studied are ca. 1 mM $Cp'_2Mo_2(CO)_6$ in neat methanol (△) and $Cp'_2Mo_2(CO)_6$ in methanol with 1% medium weight polyvinyl acetate (○).

F_{cP} by about 0.1. (For example, in *n*-octane, $\eta = 0.51$ cP and $F_{cP} = 0.33$; in cyclohexane, $\eta = 0.89$ cP and $F_{cP} = 0.48$) The results of these experiments are summarized in Table 1.

In summary of this section, the experiments above showed that the addition of 1% polymer to methanol solvent substantially changed the macroviscosity of the solution but not the recombination efficiency of a radical cage pair. It is, of course, well-known that the addition of such a small amount of macromolecule can change the macroviscosity of a solution, but the important fundamental result is that the cage recombination efficiency is insensitive to small amounts of polymeric viscogens in solution. The implication is that the solvent environment surrounding the radical cage pair is not perturbed by the small amount of polymeric viscogen.

3.4. The effect of wavelength on F_{cP}

The wavelength dependence of F_{cP} in $Cp'_2Mo_2(CO)_6$ photolysis was investigated using the steady-state method. The detailed procedure for obtaining F_{cP} by the steady-state method has been previously described [15]. In brief, values for F_{cP} were extracted from quantum yield measurements of the reaction in Eq. (1) as a function of solvent viscosity. (Solvent viscosity was modified by adding varying amounts of squalane, a non-macroscopic viscogen, to the hexanes/CCl_4 solvent [6].) The observed quantum yields (Φ_{obsd}) as a function of viscosity were then fit to Eq. (5), where c is a fitting parameter that contains k_{cP}, ϕ_{pair} is the quantum yield for formation of the radical cage pair, and ϕ_x is an offset parameter attributed to an additional electron transfer reaction [16]. (Values obtained for ϕ_x at the various wavelength of irradiation are shown in Table 2. These values indicate this reaction pathway accounts for anywhere from 6% at 546 nm to 17% at 366 nm of the bleaching of $Cp'_2Mo_2(CO)_6$.) The value for F_{cP} was then obtained by inserting the value for ϕ_{pair} into the expression $\Phi_{obsd} = \phi_{pair}[1 - F_{cP}]$

$$\Phi_{obsd} = [\phi_{pair}/(1 + \eta/c)] + \phi_x \quad (5)$$

Fig. 3 shows a typical plot for Φ_{obsd} vs. viscosity, and Fig. 4 shows the F_{cP} values that were obtained from these plots for irradiation wavelengths at $\lambda = 546$ nm (53 kcal/mol), $\lambda = 436$ nm (66 kcal/mol), $\lambda = 404$ nm (71 kcal/mol), and $\lambda = 366$ nm (78 kcal/mol). The results are summarized in Table 2, which compares the values for F_{cP} and the offset parameter, Φ_x, at the four irradiation wavelengths. The results show that F_{cP} increases from 546 nm to 436 nm (going from 0.27 ± 0.02 to 0.42 ± 0.03) but then remains more or less constant as λ decreases to 404 and 366 nm. The increase in F_{cP} as the excitation energy increases from 546 nm to the shorter wavelengths is somewhat surprising considering that the opposite behavior (i.e., a decrease in F_{cP}) was found for diatomic and triatomic molecules as the excitation energy increased. A possible explanation of this result is that the increase in F_{cP} in going from 546 nm to 436 nm can be attributed to a different photochemical excited state [18]. (The absorption band at 546 nm is assigned to a $d\pi \rightarrow \sigma^*$ transition and the band enveloping the 436 nm, 404 nm, and 366 nm wavelengths is assigned to the $\sigma \rightarrow \sigma^*$ transition.) The two electronic excited states may partition the excess energy differently among the vibrational and translational states, which could impact the velocity of separation and hence the initial separation distance of the radicals in the cage [18–20]. The observation that F_{cP} stayed constant as the excitation wavelength changed from 436 nm to 404 nm to 366 nm (all of which are in the $\sigma \rightarrow \sigma^*$ band envelope) supports this hypothesis. An alternative explanation of the "inverse" wavelength dependence is that the recombination efficiency of the radicals is affected by the speed with which the radicals impact the cage wall. When the radicals separate slowly, the solvent molecules have time to move so they can get out of the way of the separating radicals. But, when

Table 1
Comparison of F_{cP} and η for $Cp'_2Mo_2(CO)_6$ in methanol and methanol with 1% polyvinyl acetate

Solvent	F_{cP}	η (cP)
Neat methanol	0.33 ± 0.01	0.63 ± 0.03
Methanol with 1% polyvinyl acetate	0.33 ± 0.01	1.03 ± 0.04

Table 2
ϕ_x and F_{cP} (calculated for $\eta = 0.80$ cP) for the photodissociation reaction of $Cp'_2Mo_2(CO)_6$ in a hexane/squalane solvent system with 2.0 M CCl_4 added as a radical trap, as a function of irradiation wavelength

Wavelength (nm)	F_{cP} ($\eta = 0.80$ cP)	ϕ_x
546	0.27 ± 0.02	0.06 ± 0.01
436	0.42 ± 0.03	0.09 ± 0.02
404	0.45 ± 0.05	0.12 ± 0.03
366	0.40 ± 0.05	0.17 ± 0.02

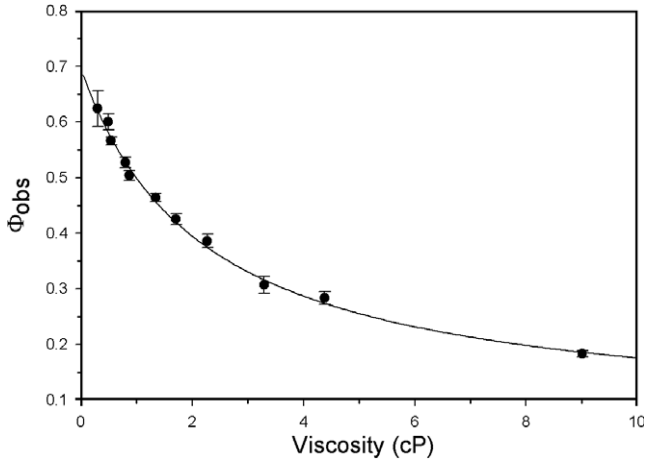

Fig. 3. Plot of Φ_{obsd} as a function of viscosity for $Cp'_2Mo_2(CO)_6$ irradiated at 545 nm. The curve represents a fit of the data to Eq. (5). For clarity, only the quantum yield data for 546 nm irradiation is shown. The error bars represent one standard deviation as determined from replicate measurements.

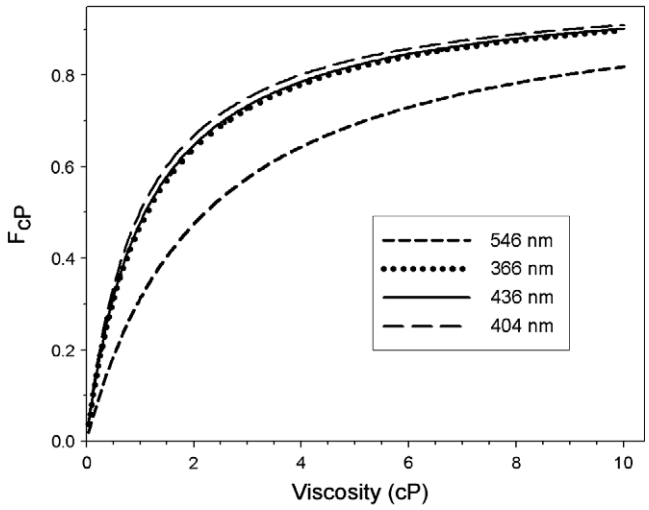

Fig. 4. F_{cP} values at 546 nm (short dashes), 436 nm (solid), 404 nm (long dashes), and 366 nm (dotted) as a function of viscosity for $Cp'_2Mo_2(CO)_6$.

the radicals separate with a greater velocity (as a consequence of the higher excitation energy) the solvent molecules have less time to move and the radicals therefore "rebound" off the cage wall more efficiently, which leads to a higher rate of radical–radical recombination. The results also showed that the ϕ_x values increased with increasing photochemical irradiation energy. This is expected for a charge-transfer-to-solvent reaction and lends additional support for the assignment of this reaction as one that originates from a charge-transfer event [17,21,22].

In summary of these results, it is apparent that the wavelength dependence of the cage effect in large polyatomic species does not necessarily mimic the wavelength dependent behavior of diatomic and simple polyatomic molecules. Care is needed, therefore, when interpreting cage effect behavior of large species based on the behavior of smaller molecules.

Acknowledgment

This work was generously supported by the NSF (CHE-0452004).

References

[1] J.P. Lorand, Prog. Inorg. Chem. 17 (1972) 207.
[2] S.A. Rice (Ed.), Comprehensive Chemical Kinetics, Elsevier, Amsterdam, Netherlands, 1985.
[3] J.L. Male, B.E. Lindfors, K.J. Covert, D.R. Tyler, J. Am. Chem. Soc. 120 (1998) 13176.
[4] J. Franck, E. Rabinowitsch, Trans. Faraday Soc. 30 (1934) 120.
[5] T. Koenig, H. Fischer, Free Radicals 1 (1973) 157.
[6] B. Otto, J. Schroeder, J. Troe, J. Chem. Phys. 81 (1984) 202.
[7] D. Madsen, C.L. Thomsen, J.A. Poulsen, S.J.K. Jensen, J. Thogersen, S.R. Keiding, E.B. Krissinel, J. Phys. Chem. A 107 (2003) 3606.
[8] R. Birdwhistell, P. Hackett, A.R. Manning, J. Organomet. Chem. 157 (1978) 239.
[9] W.L.F. Armarego, D.D. Perrin (Eds.), Purification of Laboratory Chemicals, fourth ed., Pergamon, Oxford, UK, 1997.
[10] A.B. Oelkers, L.F. Scatena, D.R. Tyler, J. Phys. Chem. A, submitted for publication.
[11] M.S. Wrighton, D.S. Ginley, J. Am. Chem. Soc. 97 (1975) 4246.
[12] T.J. Meyer, J.V. Caspar, Chem. Rev. 85 (1985) 187.
[13] A potential problem with this experiment is that, as with many metal–metal bonded dimers, M–CO bond dissociation generally becomes more prevalent as the energy of the exciting light is increased [11]. To check the experimental consequences this additional pathway might have on the measurement of F_{cP}, we compared the results of these experiments carried out under an atmosphere of CO and under an atmosphere of N_2. There were no differences in the values of F_{cP} obtained, and the measurements were henceforth carried out under N_2. (The F_{cP} analysis should be unaffected by a Mo–CO loss photoprocess as long as Mo–CO dissociation is reversible.)
[14] The kinetic traces are normalized to give A_3 a value of 1.00 ± 0.04. A_1 and A_2 values are generally dependent on the viscosity of the solvent. Typical values for A_1 and A_2 in MeOH ($\eta = 0.54 \pm 0.03$ cP) are -0.23 ± 0.02 and -0.11 ± 0.01, respectively, while in decyl alcohol ($\eta = 10.9 \pm 0.1$ cP), they are -0.30 ± 0.01 and -0.31 ± 0.01, respectively.
[15] E. Schutte, T.J.R. Weakley, D.R. Tyler, J. Am. Chem. Soc. 125 (2003) 10319.
[16] Previous work showed that measured quantum yield values at high viscosity were significantly larger than values predicted by $\sigma_{obsd} = [\phi_{pair}/(1 + \eta/c)]$. An excellent fit to this equation was achieved by adding ϕ_x; however, the addition of ϕ_x mechanistically indicates that an additional reaction pathway exists for the loss of starting material. This pathway cannot be explained by any of the previously reported radical or Mo–CO dissociation photochemical pathways and is most likely due either to the formation of an isomer or a photoinduced electron-transfer to CCl_4, mediated by a charge-transfer-to-solvent (CTTS) state (see Ref. [17] for a discussion of this point).
[17] D.A. Braden, E.E. Parrack, D.R. Tyler, Photochem. Photobiol. Sci. 1 (2002) 418.
[18] A.L. Harris, J.K. Brown, C.B. Harris, Annu. Rev. Phys. Chem. 39 (1988) 341.
[19] T. Elsaesser, W. Kaiser, Annu. Rev. Phys. Chem. 42 (1991) 83.
[20] J.C. King, J.Z. Zhang, B.J. Schwartz, C.B. Harris, J. Chem. Phys. 99 (1993) 7595.
[21] O. Traverso, F. Scandola, Inorg. Chim. Acta 4 (1970) 493.
[22] C.R. Bock, M.S. Wrighton, Inorg. Chem. 16 (1977) 1309.